optica

Spatial beam intensity shaping using phase masks on single-mode optical fibers fabricated by femtosecond direct laser writing

Timo Gissibl,* Michael Schmid, and Harald Giessen

4th Physics Institute and Research Center SCoPE, University of Stuttgart, Pfaffenwaldring 57, 70569 Stuttgart, Germany
Corresponding author: t.gissibl@pi4.uni-stuttgart.de

Submicrometer dielectric phase masks allow for the realization of the miniaturization of high-quality optical elements. In this Letter we demonstrate spatial intensity beam shaping using phase masks attached to optical single-mode fibers. The phase masks are directly fabricated onto the end facet of optical fibers using femtosecond two-photon direct laser writing, achieving, therefore, submicrometer alignment accuracy. We observe high-quality intensity patterns and find excellent agreement with simulations. Our results prove that 3D printing of diffractive micro-optics can achieve sufficient performance to enable compact devices.   © 2016 Optical Society of America

Micro-optical elements of high quality are used in a large variety of applications, such as telecommunication, sensing technology, and industrial inspection. These elements are usually integrated into systems that contain additionally electrical, mechanical, or other optical components. Therefore, it is important to further miniaturize these optical elements in order to extend the field of applications to biotechnology and medical engineering. Also, integrated fiber optical or complex lab-on-a-chip devices will become possible.

As the miniaturization of lenses is limited, diffractive elements like phase plates provide tremendous advantages. Because of their surface profile, phase plates generate a spatial phase shift and can thus be used as focusing or beam-shaping elements [1]. Conventionally, phase masks are fabricated by lithographic techniques such as gray-scale, multiple-mask, and moving-mask lithography, followed by various etching processes. These techniques are well suited for the fabrication of large-area samples, but are cost and time intensive for prototyping. In the recent past, nonlinear fabrication approaches such as femtosecond laser surface ablation were introduced [2,3]. These techniques enable maskless prototyping and production of small and medium

numbers of devices, but they still suffer from drawbacks such as low resolution and, therefore, large optical elements. Thus, femtosecond direct laser writing allows for phase masks with unprecedented feature sizes in the submicrometer range and further miniaturization of optical elements, but can also be extended to metasurfaces and metamaterials [4].

Here, we introduce 3D printed phase plates directly attached to optical single-mode fibers in order to spatially shape the emerged intensity distribution. Our phase plates are fabricated by femtosecond two-photon direct laser writing using a dip-in approach. The surface patterns of the beam-shaping phase plates are calculated using Fresnel–Huygens diffraction theory. By analyzing the optical performance of the diffractive optical elements, we demonstrate the viability of the fabrication technique for producing compact integrated optical elements.

Femtosecond 3D direct laser writing is additionally well suited for the manufacturing of refractive free-form surfaces, compound lenses, and photonic crystal structures with submicrometer feature sizes. As a result, it is possible to manufacture optical elements to control the light propagation, including polarization and intensity [5]. Therefore, our method is not limited to the presented diffractive optical elements here.

To manufacture diffractive optical elements directly onto the end facet of optical fibers, further approaches have recently been proposed. These are techniques such as interference lithography [6], photolithography [7], electron-beam lithography [8], and focused ion-beam milling [9]. Our method establishes a fast, simple, and straightforward fabrication alternative to the listed techniques with various advantages.

Figure 1(a) depicts a phase plate for beam intensity shaping directly attached to the end facet of an optical single-mode fiber (SM 780HP, Thorlabs). The optical phase plate consists of a base and a diffractive element with a total diameter of 17.6 μm. The actual diffractive element has a diameter of only 4.4 μm and is precisely centered on the fiber core. Figure 1(b) displays a detailed scanning electron image of the phase mask.

The surface profile of our phase mask is obtained by numerically solving the Huygens–Fresnel diffraction integral in two dimensions. To reach the target intensity distribution, the structure of the phase masks is stepwise improved by an iterative optimization algorithm [10], which is implemented in MATLAB by
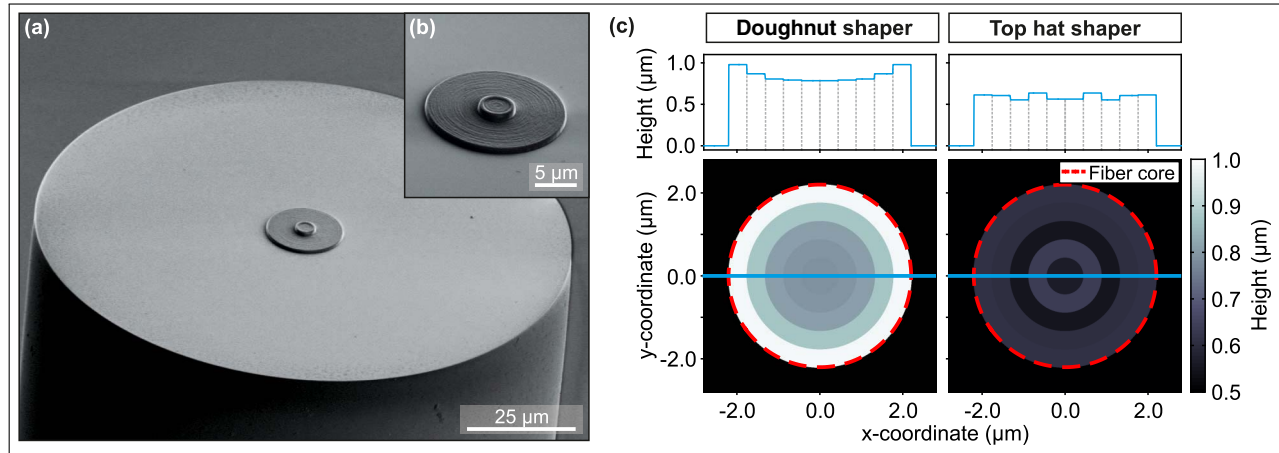
Fig. 1. (a) Scanning electron microscope image of a diffractive optical element attached to the end facet of an optical fiber. The diffractive phase plate is fabricated ring-by-ring using 3D direct laser writing. (b) Zoom-in view of the phase mask sitting on a direct laser written base. (c) Structure design of diffractive optical elements for shaping a doughnut or a top-hat intensity distribution. Each structure consists of five rings with heights below 1 μm and widths of 440 nm.

utilizing rotational symmetry [11]. The refractive index of the exposed photoresist is assumed to be 1.513 for all simulations. This value corresponds to the value of a comparable photoresist at 800 nm wavelength. The mode field radius of our single-mode optical fiber is set to 2.45 μm, which is obtained by modal theory with refractive indices of 1.4598 and 1.4537 for the core and cladding materials, respectively [12]. For the mode theory calculations, a core diameter of the optical fiber of 4.4 μm is used. The radial integration range for solving the Huygens–Fresnel diffraction integral is determined to –6 to 6 μm, centered around the fiber core. The design wavelength is set to be 808 nm, corresponding to our laser diode. The propagation distance between target and phase mask (fiber end face) is chosen to be 10 mm.

Every phase mask consists of five rings, where each ring has a width of 440 nm and is limited to a maximum height of 2 μm in simulation. As intensity distribution targets, doughnut-shaped and circular top-hat intensity distributions are chosen. The numerical simulations of the circular phase masks for the doughnut shaper result in surface relief heights of 785, 793, 805, 868, and 979 nm, beginning at the center. The top hat shaper is described by heights of 563, 636, 554, 606, and 613 nm.

Figure 1(c) shows the height profiles of the calculated phase masks for shaping a doughnut and a top-hat intensity distribution, respectively. The target intensity distributions of the two beam-shaping phase masks and the corresponding results of the simulations are shown in Fig. 2(a). The simulated beam profile deviates in the case of the top hat from the target, as only a limited number of rings are used for discretization purposes.

The simulated evolutions of the shaped intensity distribution as a function of propagation distance are shown in Fig. 2(b). In both cases, the desired target intensity profiles are formed in the first few millimeters behind the fiber end. Afterward, the shaped intensity distributions propagate as known for beam propagation of optical single-mode fibers as a divergent beam. The shaped intensity distributions are retained over the whole simulated propagation distance.

Two-photon polymerization allows for the fabrication of optical elements with feature sizes below 100 nm [13,14]. Therefore, this technique is perfectly suited for the fabrication

of phase masks with feature sizes in the submicrometer range. We use a commercially available two-photon 3D laser lithography system (Nanoscribe GmbH) at $\lambda = 780$ nm for fabricating the diffractive elements. The phase masks are directly manufactured onto the end facets of optical single-mode fibers by the dip-in technique [15]. A droplet of the photoresist IP-Dip (Nanoscribe GmbH) is placed onto the objective lens, and, subsequently, the fiber is dipped into this droplet of photoresist. To accurately center the fiber core with respect to the writing beam, the core is aligned by illuminating the opposite fiber end facet and adjusting the fiber position using a magnified CCD image. During the fabrication process, the laser is laterally moved via galvanometric mirrors. Ultraprecise piezo actuators execute the axial movement. Optical single-mode fiber pieces (SM 780HP, Thorlabs) with lengths of 15 to 20 cm are used for the fabrication.

The phase masks are fabricated ring-by-ring beginning at the center. Each 440 nm broad ring consists of five rings with the same height but different radii. By stacking numerous writing trajectories on top of each other, every ring is created. The layer-by-layer distance is 50 nm. Each circular trajectory consists of several points with 15 nm distance and begins at a random position on the circle so as to create homogeneous structures.

As it is quite challenging to locate the interface of the fiber end facet with an accuracy of tens of nanometers, a base with a height of 500 nm and a total diameter of 17.6 μm is fabricated beneath the phase mask [Figs. 1(a) and 1(b)].

After the fabrication process, the unexposed photoresist is removed by a developing bath for 15 min in mr-dev 600 (micro resist technology GmbH) and a subsequent rinse with isopropanol. Since the surface of the fiber end facet and the structure is very small, no drying is necessary. We characterize the written phase mask optically by coupling light of a laser diode with an operating wavelength of 808 nm (LP808-SF30, Thorlabs) into the fiber pieces. The emerged light is analyzed by taking pictures at several distances behind the fiber end with a CCD camera (GC 2450C, Allied Vision Technologies). Therefore, the camera is moved by a linear translation stage (PI miCos GmbH) in 250 μm steps. The absolute distance between fiber end and
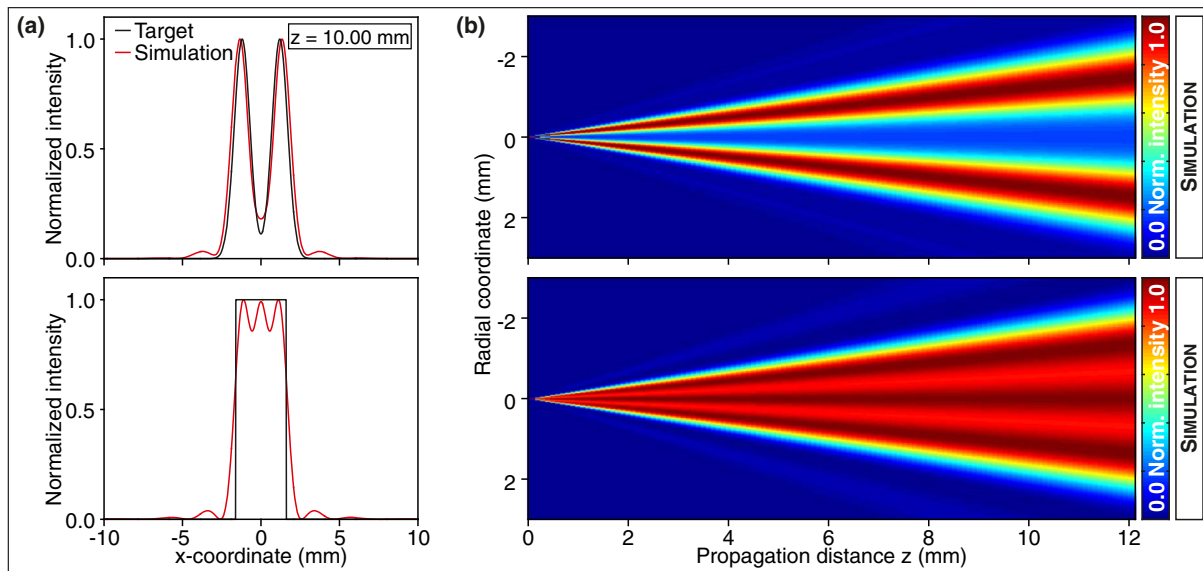
Fig. 2. Simulations of the normalized intensity distribution of the doughnut and top-hat shaping diffractive optical elements, respectively. (a) Cross sections of the simulated intensity distribution of the doughnut-shaped and the top-hat-shaped beam profiles at a propagation distance z of 10 mm. Additionally, the target intensity distributions are shown. (b) Simulations of the intensity distribution at different distances after the fiber end obtained by numerically solving the Huygens–Fresnel diffraction integral in two dimensions for the two different diffractive structure designs.

CCD chip is calibrated by comparing the measured profiles with the simulated ones.

Figure 3(a) shows the normalized intensity distribution of a doughnut-shaping phase mask in a distance of 5 mm behind the fiber end. The emerged Gaussian intensity distribution of the single-mode fiber is completely redistributed in order to form the beam profile within a few millimeters' propagation distance. Additionally, the cross sections in the x and y directions are depicted. Figure 3(b) displays the intensity distribution of the top-hat shaping phase mask with the corresponding cross sections. Both the doughnut and top-hat shapers exhibit high-quality performance.

Figure 4 depicts the experimental results for the propagation of the intensity distribution behind the phase mask. The measured beam propagation of the doughnut-shaping phase mask in Fig. 4(a) is in excellent agreement with the simulations in Fig. 2(b). At each z position of the evolution plot, the beam profile is calculated as the average of the beam profile in the
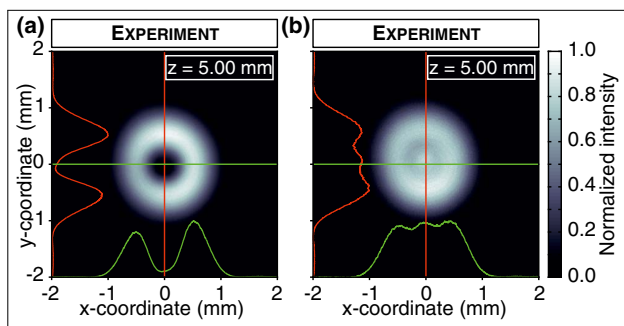

Fig. 3. Measured intensity distribution for (a) the doughnut and (b) the top-hat shaping diffractive optical element at a distance of 5 mm behind the fiber end. The mode images are obtained by taking pictures with a CCD camera.
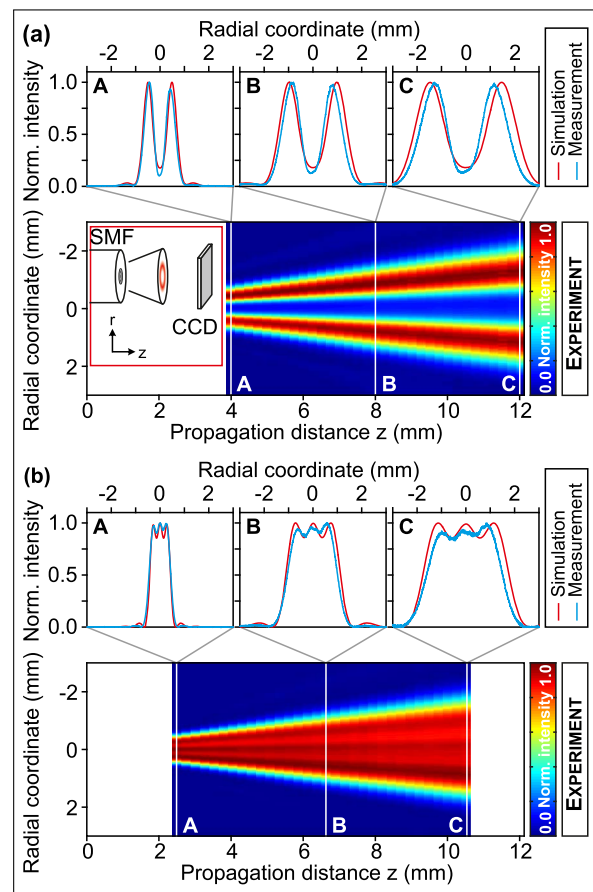

Fig. 4. Measurement of the intensity distribution at different distances behind the fiber end for (a) the doughnut and the (b) top-hat shapers. The measurement is compared to the simulation at several positions.

x and y directions. The normalized intensity profiles of the cross sections at 4, 8, and 12 mm behind the fiber end, marked as positions A, B, and C, show excellent agreement with the simulations, as well. Figure 4(b) depicts the propagation of the intensity behind the top-hat shaping phase mask. The two small dips in the measured intensity profiles can be seen in the simulated intensity distributions, too. There is again an excellent agreement between the measured and the simulated intensity distributions, which can be seen in the cross sections at distances of 2.5, 6.5, and 10.25 mm, marked as positions A, B, and C in the plots, as well.

The total degree of transmittance of phase masks on fibers with lengths of about 20 cm can reach up to 46.8%. As the intensity shaping phase masks are directly fabricated onto the cores of optical fibers, the alignment is tremendously accurate, and, therefore, the intensity shape is highly symmetric. Three-dimensional direct laser writing fabrication is well suited for the fabrication of optical structures with feature sizes in the submicrometer range that exhibit outstanding fabrication qualities. To demonstrate the high reproducibility of this fabrication scheme, we fabricate phase masks with different numbers of rings. All of them are directly attached to the end facet of a single-mode optical fiber and are designed to have the same target intensity distribution. We choose the doughnut-shaped intensity distribution introduced in Fig. 2(a) as a target profile. We find excellent agreement between the different measurements (see Supplement 1). This is also confirmed by the corresponding numerical calculations using Fresnel–Huygens diffraction. As they have different numbers of rings, the phase mask profiles are quite different, which confirms the high fabrication quality and shape accuracy of the phase masks.

Additionally, we check fabrication influences on the quality of the phase masks. We manufactured phase masks, on the one hand, ring-by-ring as mentioned above and, on the other hand, layer-by-layer. Both fabrication methods give high-quality structures, and, therefore, there is an excellent agreement between the two manufacturing methods (see Supplement 1).

In conclusion, we demonstrated various optical phase masks with submicrometer feature sizes, enabling spatial intensity shaping, directly fabricated onto single-mode optical fibers. The optical elements are manufactured using femtosecond 3D direct laser writing with a dip-in approach. As this technique enables feature sizes below 100 nm, unprecedented diffractive elements with diameters in the low micrometer range are feasible. Thus, the intensity distribution that emerges from an optical fiber can be spatially redistributed. Additionally, direct laser writing provides a fabrication technique that allows for the fabrication of other optical elements, such as refractive free-form, reflective,

or polarization controlling optics. Our method extends the realm of additive optical manufacturing into micro- and nano-optics and opens a new field for integrated fiber optical or complex lab-on-a-chip devices. Also, specific spatial modes and higher orbital angular momentum states in multimode fibers can easily be generated.

See Supplement 1 for supporting content.

REFERENCES

1. V. A. Soifer, *Methods for Computer Design of Diffractive Optical Elements* (Wiley, 2002).
2. M. Mizoshiri, H. Nishiyama, J. Nishii, and Y. Hirata, Appl. Phys. A **98**, 171 (2010).
3. R. M. Vázquez, S. M. Eaton, R. Ramponi, G. Cerullo, and R. Osellame, Opt. Express **19**, 11597 (2011).
4. N. Yu and F. Capasso, Nat. Mater. **13**, 139 (2014).
5. M. Malinauskas, M. Farsari, A. Piskarskas, and S. Juodkazis, Phys. Rep. **533**, 1 (2013).
6. S. Tibuleac, D. Wawro, and R. Magnusson, "Resonant diffractive structures integrating waveguide-gratings on optical fiber endfaces," in *12th Annual Meeting IEEE Lasers and Electro-Optics Society (LEOS)* (IEEE, 1999), p. 874.
7. E. G. Johnson, J. Stack, T. J. Suleski, C. Koehler, and W. Delaney, Appl. Opt. **42**, 785 (2003).
8. M. Prasciolu, D. Cojoc, S. Cabrini, L. Businaro, P. Candeloro, M. Tormen, R. Kumar, C. Liberale, V. Degiorgio, A. Gerardino, G. Gigli, D. Pisignano, E. Di Fabrizio, and R. Cingolani, Microelectron. Eng. **67–68**, 169 (2003).
9. F. Schiappelli, R. Kumar, M. Prasciolu, D. Cojoc, S. Cabrini, M. De Vittorio, G. Visimberga, A. Gerardino, V. Degiorgio, and E. Di Fabrizio, Microelectron. Eng. **73–74**, 397 (2004).
10. J. C. Lagarias, J. A. Reeds, M. H. Wright, and P. E. Wright, SIAM J. Optim. **9**, 112 (1998).
11. S. Thiele, A. Seifert, and A. M. Herkommer, Opt. Express **22**, 13343 (2014).
12. J. A. Buck, *Fundamentals of Optical Fibers*, 2nd ed. (Wiley, 2004).
13. J. Fischer and M. Wegener, Laser Photon. Rev. **7**, 22 (2013).
14. Z. Gan, Y. Cao, R. A. Evans, and M. Gu, Nat. Commun. **4**, 2061 (2013).
15. T. Bückmann, N. Stenger, M. Kadic, J. Kaschke, A. Frölich, T. Kennerknecht, C. Eberl, M. Thiel, and M. Wegener, Adv. Mater. **24**, 2710 (2012).